THE ASTROPHYSICAL JOURNAL, 444:810–817, 1995 May 10

MASSES OF DA WHITE DWARFS WITH GRAVITATIONAL REDSHIFT DETERMINATIONS

P. BERGERON,[1] JAMES LIEBERT,[2] AND M. S. FULBRIGHT[2]
Received 1994 August 5; accepted 1994 November 15

ABSTRACT

We estimate effective temperatures and surface gravities for 35 DA white dwarfs with previously published gravitational redshifts, with known systemic velocities based on a companion or cluster membership. The spectroscopically determined mass estimates are then compared with those inferred from the redshifts, using in both cases the evolutionary models of Wood.

We find that when the redshift velocities from Wegner & Reid are excluded from the sample, the gravitational redshift and spectroscopic masses agree well within 1 σ, suggesting that the theoretical assumptions used in the model spectra are sound. However, when determinations from this last reference are included in the analysis, strong discrepancies arise: for the sample of stars cooler than $T_{\rm eff} \sim 12{,}000$ K, the scatter in the results from the two methods is much larger than for the hotter stars, and the gravitational redshift masses then appear significantly larger than the spectroscopic masses at all temperatures.

An analysis of the ZZ Ceti star G117-B15A yields good agreement with the gravitational redshift determination only if the ML2 parameterization of the mixing-length theory of convection is used in the spectroscopic analysis. The spectroscopic masses alone reveal that cool ($T_{\rm eff} < 12{,}000$ K) DA white dwarfs appear to have larger masses, a result which has been interpreted in the past as conclusive evidence for helium enrichment due to the occurrence of convective mixing.

Subject headings: gravitation — stars: fundamental parameters — white dwarfs

1. INTRODUCTION

The gravitational redshift is one of Einstein's original tests of the theory of general relativity, and the first confirmatory measurements were of the white dwarf star Sirius B (Adams 1925). Assuming that general relativity has passed this test, one can now use the redshift measurement to determine the ratio of mass to radius of a white dwarf, provided that the systemic radial velocity of the star is known—for those in binary systems or star clusters. One can generally also assume that the intrinsic mass-radius relation for white dwarfs of a given composition is known fairly accurately—from detailed evolutionary calculations which account for a swelling of the white dwarf radius due to finite temperature effects (Wood 1990). One can then determine both the mass and radius of a given star.

There are several drawbacks to using gravitational redshifts to estimate the mass distribution of samples of white dwarfs. First, the stars have absorption lines that are generally quite broad, due to the extreme pressure broadening. Fortunately, those of the dominant DA spectral type may have fairly narrow non-LTE cores of the Hα line (Greenstein et al. 1977). Nevertheless, the high spectral resolution necessary for a meaningful measurement excludes faint stars and still requires a large telescope. Moreover, the lines of helium and other elements detected in those of non-DA spectral types are broader than the hydrogen lines and often are not measurable at all. The neutral helium lines of the spectra of DB stars are subject to uncertain pressure shifts (Greenstein & Trimble 1967; Koester 1987). Finally, only a fraction of even the DA stars are members of binary systems or clusters, such that the systemic radial velocity of the star may be subtracted from the observed radial velocity to obtain the gravitational redshift velocity. We note, however, that even though this fraction is relatively small, there are still $\sim$200 common proper motion pairs with classified DA white dwarf components.

A more general way of estimating a mass of a white dwarf is to fit line profiles, which are sensitive to the temperature and surface gravity, using model atmospheres. For large samples of DA stars, the simultaneous fits to accurate Balmer line profiles measured with spectrographs using CCD detectors at modest spectral resolution have yielded parameters with quite small internal errors (Bergeron, Saffer, & Liebert 1992a, hereafter BSL). The surface gravity and evolutionary models yield independent ratios of mass to radius (or the square of the radius), permitting the determination of each.

BSL deliberately limited their sample to stars with estimated $T_{\rm eff}$ values of 15,000 K or higher. The principal reason for this choice is the onset of atmospheric convection below this temperature, and the evidence that the derived stellar/atmospheric parameters depend on the parameterization of the mixing-length theory (Bergeron, Wesemael, & Fontaine 1992b). Further difficulties would be faced below the ZZ Ceti pulsational instability strip, near 11,500 K, where a similar analysis led to the conclusion either that stars have higher gravities and masses than their hotter counterparts, or that a substantial amount of helium is present in the atmosphere (Bergeron et al. 1990). However, it cannot be ruled out at this stage that some uncertainty in the treatment of the physics of the cooler stars is the cause of this systematic gravity offset (see below, however).

Even for a sample chosen in the optimum temperature range to avoid these problems, however, the absolute accuracy of the technique depends on the accuracy of the occupation probability formalism for excited levels of the hydrogen atom (Hummer & Mihalas 1988; Bergeron, Wesemael, & Fontaine 1991)—that is, the "quenching" especially of upper levels due to the

[1] Département de Physique, Université de Montréal, C.P. 6128, Succ. Centre-ville, Montréal, Québec, Canada, H3C 3J7; bergeron@astro.umontreal.ca.
[2] Steward Observatory, University of Arizona, Tucson, AZ 85721; liebert, msf@as.arizona.edu.

presence of nearby charges in a dense plasma—and on the treatment of Stark broadening (Bergeron 1993). BSL (see also Bergeron 1993) found that an arbitrary modification of the published formulations was required in order to yield good agreement in $T_{\rm eff}$ and $\log g$ between the higher and lower Balmer lines.

It is important, therefore, to test the results of the line profile fits by comparing parameters determined from this method with those available from other techniques, of which the gravitational redshift is an important case. BSL compared their inferred masses with those derived from published gravitational redshift determinations. It was reassuring that the mean masses from the two determinations agreed to within $0.02\,M_{\odot}$, and that the white dwarfs analyzed in the Hyades and Pleiades clusters had higher masses than the average, as expected, because they evolved from more massive progenitor stars than do the typical field white dwarfs. There were, however, only 11 stars having both kinds of determinations (BSL, their Table 4).

In the last few years, additional gravitational redshift determinations have been published. The purpose of this paper is to present new spectrophotometric observations and stellar atmospheres fits for these stars, in order to increase the sample common to both analyses. The new sample, however, includes mostly stars cooler than the BSL limit of 15,000 K. In addition to confirming the validity of our model spectra for hotter stars, the original goals of this project include the use of cooler stars to determine (1) the appropriate parameterization of the mixing-length theory in the $T_{\rm eff}$ range where convection is not adiabatic, and (2) the nature of the different derived parameters and/or theoretical problems with DA white dwarfs cooler than the ZZ Ceti instability strip.

2. SPECTROSCOPIC OBSERVATIONS AND LINE FITS

The telescope (Steward 2.3 m), spectrograph parameters, CCD detector, and observational techniques used for this project are essentially the same as those utilized for the BSL study, so details need not be repeated here. For reasons outlined in § 3, the so-called ML2 parameterization of the mixing-length theory (see Bergeron et al. 1992b for the use of this nomenclature) is used throughout our analysis. Twenty-three new DA stars with published gravitational redshifts and north of declination of approximately −30 degrees were observed on 1991 November 2–3 and 1992 March 25–26, increasing the sample to 3 times that of BSL. As an external check of our method, the 11 stars studied in BSL were reobserved and are reanalyzed here as well. The spectrum of G191-B2B is taken from Bergeron et al. (1994). The optical spectra for the 35 DA stars with gravitational redshift measurements are displayed in Figure 1.

The method of normalizing the continuum and simultaneously fitting all hydrogen lines except Hα is also discussed at length in BSL and earlier papers. Illustrative examples of fits

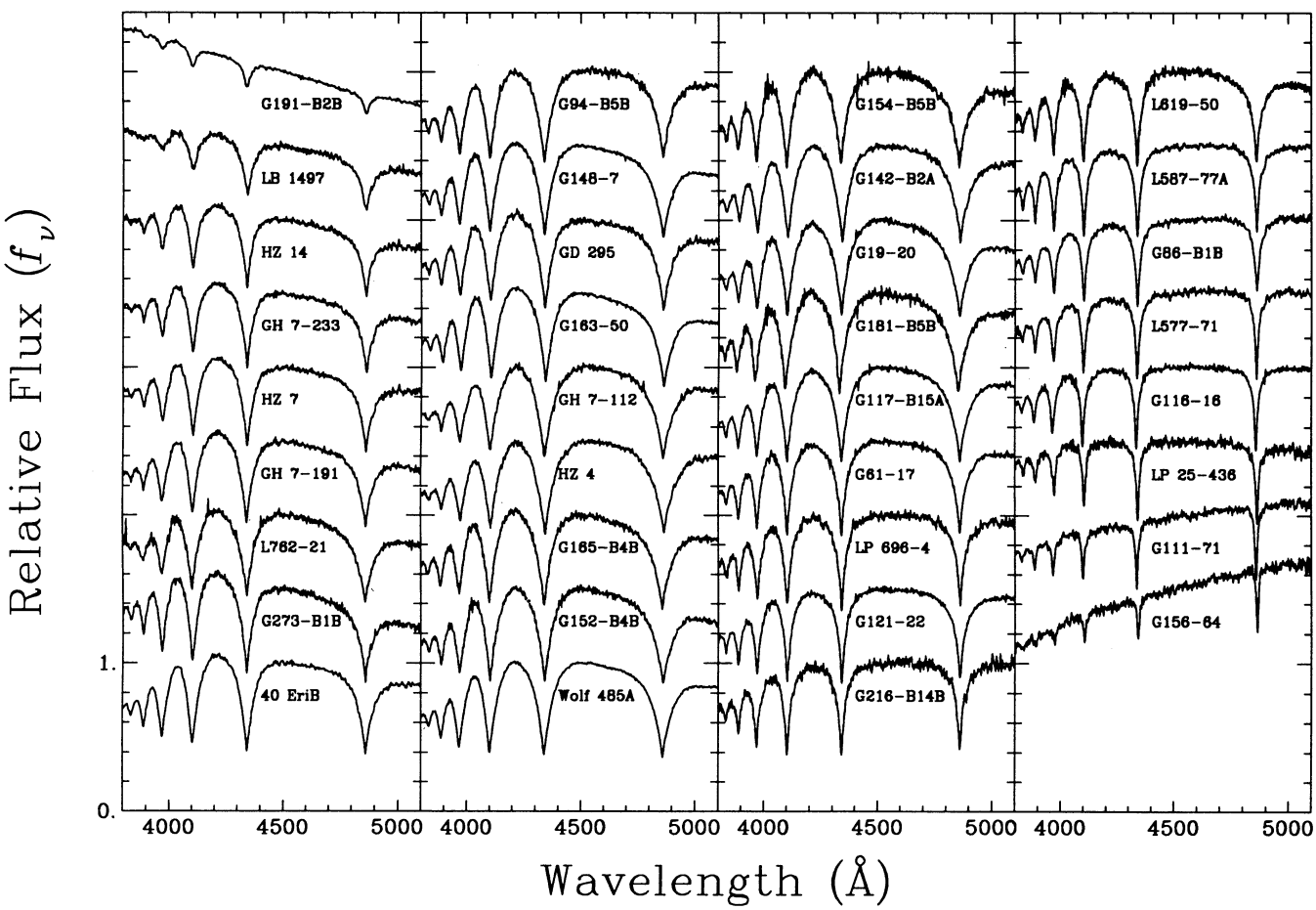

FIG. 1.—Optical spectra for the sample of 35 DA stars with gravitational redshift measurements. The spectra are normalized to unity at 4500 Å and are shifted vertically by 0.5 for clarity. The effective temperature decreases from upper left to bottom right. The spectral resolution of this sample is ~6 Å (FWHM).

for the hotter stars are shown in BSL. Additional fits for the cooler stars are displayed in Figure 2; G67-23 has no gravitational redshift measurement but the fit is used for a comparison discussed below. The resulting $T_{\rm eff}$, log g, and spectroscopic mass estimates ($M_{\rm Sp}$) from fits to each observed star are listed in Table 1, along with the published gravitational redshift velocities, the inferred gravitational redshift masses ($M_{\rm GR}$), and the references; the atmospheric parameters for G191-B2B are taken from Bergeron et al. (1994). Quantities in parentheses are the error estimates; the uncertainties of ($M_{\rm GR}$) have been derived from the errors of the velocity measurements while the spectroscopic mass uncertainties are internal errors of the fitting procedure only. For cases where a star has two published redshift determinations, it is listed twice in Table 1.

In order to take into account finite-temperature effects, we have used in Table 1 the evolutionary models of Wood (1990) to derive the spectroscopic masses from the log g determinations. Similarly, the gravitational redshift masses have been redetermined from the published values of the velocities using the same evolutionary models. These models have a carbon-core composition, a helium layer of $M_{\rm He} = 10^{-4} M_*$, and no hydrogen layer. As discussed in BSL, the mass of the hydrogen layer remains the largest source of uncertainty in deriving spectroscopic masses. For instance, if models with thick hydrogen layers ($M_{\rm H} = 10^{-4} M_*$) are used instead, the spectroscopic masses could be larger by as much as 0.04 $M_\odot$. To evaluate the corresponding uncertainties on our analysis, we have derived spectroscopic masses using new evolutionary models with thick hydrogen layers kindly provided to us by M. A. Wood. Fortunately, it turns out that gravitational redshift masses are increased by similar amounts. For example, the masses of HZ 7 in Table 1 increase to values of $M_{\rm GR} = 0.686\ M_\odot$ and $M_{\rm Sp} = 0.652\ M_\odot$. Hence, the difference between the gravitational redshift mass and the spectroscopic mass is 0.034 $M_\odot$ with thick hydrogen models, a value comparable to 0.042 $M_\odot$ when models with no hydrogen layer are used (Table 1). Therefore, we conclude that although the absolute values of the masses derived from spectroscopy or gravitational redshift measurements depend on the assumption about the thickness of the hydrogen layer, the *mass difference* between both techniques remains unaffected. In particular, plots similar to Figures 4 and 5, below, obtained with thick hydrogen models are practically undistinguishable from those displayed here with no hydrogen layer.

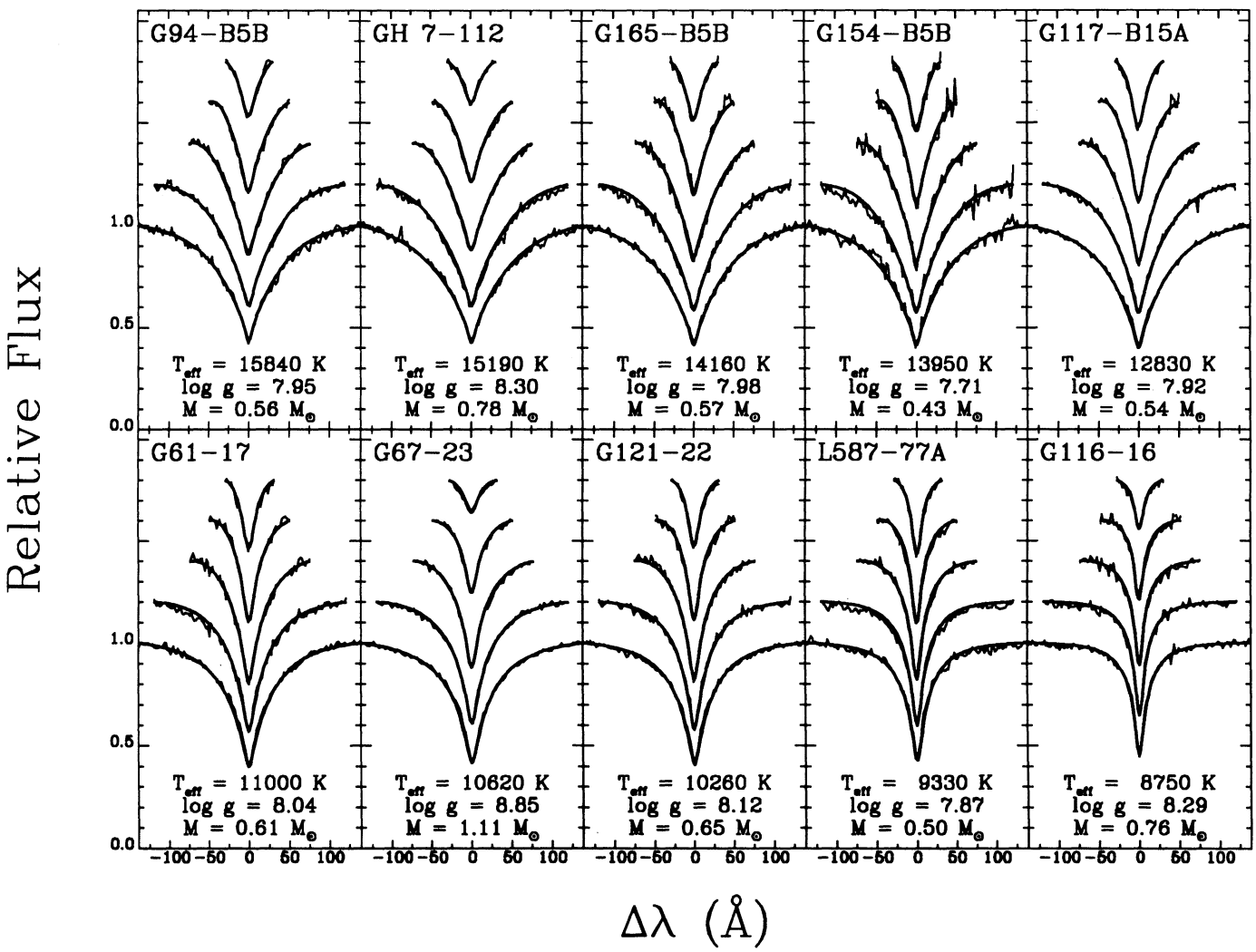

FIG. 2.—Fits to the individual Balmer lines (Hβ to H8 from bottom to top) for some DA stars with gravitational redshift measurements, except for G67-23, which is discussed in § 3. In each panel, the lines are normalized to a continuum set to unity, and offset vertically by a factor of 0.2.

TABLE 1

COMPARISON WITH GRAVITATIONAL REDSHIFT MEASUREMENTS

Name	WD	$T_{\rm eff}$ (K)	log g	$v_{\rm GR}$ (km s^{-1})	$M_{\rm GR}/M_\odot$	$M_{\rm Sp}/M_\odot$	Notes
G94-B5B	0220+222	15840	7.95	70.0 (6.0)	0.940 (0.037)	0.561 (0.031)	1
LP 591-117	0251−008	...	...	25.0 (7.0)	...	...	1, 2
L587-77A	0326−273	9330	7.87	36.1 (3.2)	0.657 (0.035)	0.504 (0.030)	3
LB 1497	0349+247	31660	8.78	84.0 (9.0)	1.025 (0.043)	1.084 (0.029)	4
HZ 4	0352+096	14770	8.16	33.3 (3.8)	0.632 (0.042)	0.687 (0.035)	5
GH 7-112	0406+169	15190	8.30	48.7 (4.5)	0.783 (0.039)	0.776 (0.036)	5
40 Eri B	0413−077	16570	7.86	23.9 (3.0)	0.520 (0.040)	0.516 (0.029)	6
40 Eri B	0413−077	16570	7.86	26.5 (1.5)	0.554 (0.019)	0.516 (0.029)	7
GH 7-191	0421+162	19570	8.09	36.1 (3.4)	0.669 (0.036)	0.652 (0.033)	5
GH 7-233	0425+168	24420	8.11	30.9 (2.5)	0.617 (0.028)	0.673 (0.033)	5
GH 7-233	0425+168	24420	8.11	35.7 (3.8)	0.670 (0.040)	0.673 (0.033)	1
HZ 7	0431+125	21340	8.04	35.6 (7.3)	0.665 (0.077)	0.623 (0.032)	5
HZ 14	0438+108	27390	8.07	21.8 (6.4)	0.510 (0.086)	0.652 (0.032)	5
HZ 14	0438+108	27390	8.07	29.7 (5.8)	0.608 (0.067)	0.652 (0.032)	1
G191-B2B	0501+527	64100	7.69	19.0 (4.0)	0.538 (0.043)	0.548 (0.017)	8
G86-B1B	0518+333	9140	8.30	20.0 (8.0)	0.454 (0.118)	0.767 (0.037)	1
GD 295	0810+234	15220	7.99	38.0 (7.0)	0.682 (0.072)	0.579 (0.031)	1
G111-71	0816+387	7710	8.15	34.0 (11.0)	0.632 (0.125)	0.669 (0.035)	1
G116-16	0913+442	8750	8.29	83.0 (12.0)	1.009 (0.060)	0.759 (0.037)	1
G117-B15A	0921+354	12830	7.92	29.0 (6.0)	0.579 (0.074)	0.537 (0.031)	1
G163-50	1105−048	15070	7.83	20.1 (3.2)	0.465 (0.046)	0.493 (0.028)	3
G163-50	1105−048	15070	7.83	19.7 (3.0)	0.459 (0.043)	0.493 (0.028)	6
G148-7	1143+321	15480	7.97	27.0 (3.0)	0.558 (0.038)	0.574 (0.031)	6
G121-22	1147+255	10260	8.12	100.0 (6.0)	1.084 (0.023)	0.651 (0.035)	1
G61-17	1244+149	11000	8.04	27.0 (3.0)	0.552 (0.038)	0.605 (0.033)	1
Wolf 485A	1327−083	14100	7.93	24.9 (3.2)	0.529 (0.042)	0.544 (0.030)	3
Wolf 485A	1327−083	14100	7.93	24.9 (3.0)	0.529 (0.039)	0.544 (0.030)	6
L762-21	1334−160	18580	8.32	51.2 (12.0)	0.808 (0.099)	0.797 (0.036)	3
L762-21	1334−160	18580	8.32	55.0 (9.0)	0.838 (0.070)	0.797 (0.036)	1
L619-50	1348−273	10080	8.17	23.3 (5.0)	0.502 (0.069)	0.682 (0.036)	3
G165-B5B	1354+340	14160	7.98	22.0 (3.0)	0.490 (0.042)	0.573 (0.032)	1
G66-35/36	1449+003	...	...	42.0 (3.0)	...	...	1, 9
G152-B4B	1555−089	14100	7.88	36.0 (5.0)	0.661 (0.054)	0.519 (0.029)	1
G181-B5B	1706+332	13600	7.79	26.0 (8.0)	0.543 (0.104)	0.470 (0.027)	1
G240-47	1710+683	...	...	34.0 (3.0)	...	...	1, 10
G19-20	1716+020	13620	7.79	22.0 (6.0)	0.489 (0.084)	0.470 (0.027)	3
G19-20	1716+020	13620	7.79	20.4 (3.0)	0.466 (0.043)	0.470 (0.027)	6
G154-B5B	1743−132	13950	7.71	24.5 (3.0)	0.524 (0.040)	0.431 (0.025)	6
G140-B1B	1750+098	...	...	31.0 (6.0)	...	...	1, 11
G142-B2A	1911+135	14040	7.84	27.4 (3.0)	0.561 (0.037)	0.499 (0.029)	6
G142-B2A	1911+135	14040	7.84	44.0 (4.0)	0.741 (0.037)	0.499 (0.029)	1
LP 696-4	2044−043	10470	8.11	19.0 (8.0)	0.440 (0.120)	0.647 (0.035)	1
LP 25-436	2047+809	8440	8.52	35.0 (5.0)	0.644 (0.056)	0.916 (0.036)	1
G156-64	2253−081	7160	8.43	27.0 (4.0)	0.548 (0.052)	0.857 (0.037)	1
G216-B14B	2258+406	9860	8.20	55.0 (6.0)	0.832 (0.047)	0.701 (0.036)	1
G273-B1B	2350−083	18940	7.81	31.0 (3.0)	0.612 (0.035)	0.493 (0.027)	1
L577-71	2351−335	8780	8.29	27.0 (3.0)	0.549 (0.038)	0.760 (0.037)	1

NOTES.—(1) Wegner & Reid (1991). (2) Not observed spectroscopically. (3) Koester (1987). (4) Wegner, Reid, & McMahan (1991). (5) Wegner, Reid, & McMahan (1989). (6) Wegner & Reid (1987). (7) Koester & Weidemann (1991). (8) Reid & Wegner (1988). (9) Nondegenerate pair (I. N. Reid, private communication). (10) Too faint (V = 17.1). (11) Only Hα visible.

In Figure 3 we compare the $T_{\rm eff}$ and log g determinations for the 11 stars in common with BSL. Also reproduced on the same plot are the results of the multiple observations of the 19 DA stars from Table 2 of BSL; these multiple measurements were used by BSL to evaluate the external errors in temperature ($\sim$350 K), surface gravity ($\sim$0.05 in log g), and mass (0.03 $M_\odot$). The results of Figure 3 indicate that our current estimates are totally compatible with those of BSL, and thus, that the uncertainties of the fitted parameters are comparable as well.

3. COMPARISON OF MASS ESTIMATES

For models cooler than 15,000 K, the determinations of $T_{\rm eff}$ and log g depend on the parameterization of the mixing-length theory (Bergeron et al. 1992b). As discussed above, one of the goals of this project was to use gravitational redshift measurements to constrain the convective efficiency in DA stars. Unfortunately, most stars analyzed here with convective atmospheres are cooler than the red edge of the ZZ Ceti instability strip ($T_{\rm eff} \sim$ 11,500 K). Since convective mixing may have occurred for these cooler DA stars (Bergeron et al. 1990), the measured surface gravities cannot be translated directly into masses. Indeed, Bergeron et al. (1991) have shown that it is not possible to separate the pressure effects originating from an increased helium abundance from those stemming from an increased surface gravity. Since in the following we assume that all white dwarfs have pure hydrogen atmospheres, the spectroscopic masses determined for stars cooler than 11,500 K represent only *upper limits* to the real stellar mass.

Therefore, only DA stars below 13,500 K where convection

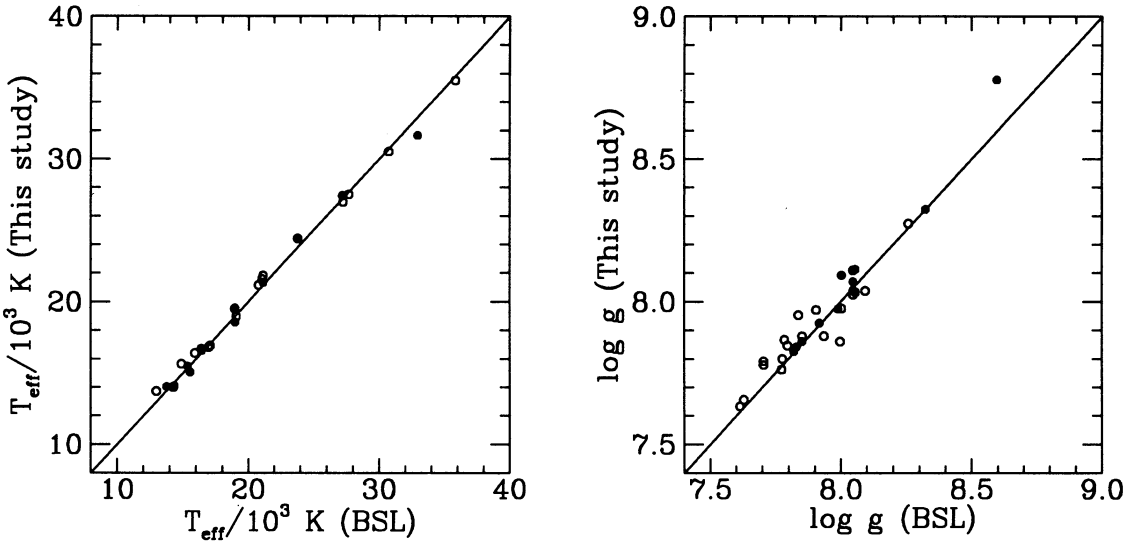

FIG. 3.—T_{eff} and log g determinations obtained in this study compared to those of BSL for the 11 DA stars in common (*filled circles*). The open circles represent the multiple measurements of 19 DA stars taken from Table 2 of BSL; note that the labels are meaningless for this comparison since both determinations come from BSL. The results illustrate that the reproducibility of both studies is comparable.

carries an important fraction of the total flux (Bergeron et al. 1991), and yet above 11,500 K where the assumption of a pure hydrogen composition is well founded, can be used to study the influence of the convective efficiency on the determination of the atmospheric parameters of DA white dwarfs. Consequently, ZZ Ceti stars are best suited to accomplish this task. G117-B15A, a well-known ZZ Ceti star, has a gravitational redshift measurement obtained by Wegner & Reid (1991, hereafter WR91), and is thus included in our analysis. The gravitational redshift mass derived for this object is $M_{GR} = 0.58 \pm 0.07\ M_\odot$, while the spectroscopic masses are $M_{Sp} = 0.69$, 0.54, and $0.47 \pm 0.03\ M_\odot$ for the ML1, ML2, and ML3 parameterization of the mixing-length theory, respectively. Even though we have only one star for which this comparison can be performed, our result suggests that the ML2 version is to be preferred. This last result is entirely consistent with the detailed analysis of a sample of 18 ZZ Ceti stars by Bergeron et al. (1995), who find that the ML2 parameterization gives a mean mass which is comparable to that of the warmer BSL sample, while ML1 and ML3 yield means which are in strong disagreement (see also Bergeron et al. 1992b). Koester, Allard, & Vauclair (1994) also conclude that a relatively high convective efficiency is required in order to achieve a satisfactory fit to the ultraviolet (FOS/*HST*) energy distribution of G117-B15A.[3] Detailed hydrodynamic calculations also indicate that the convective efficiency in ZZ Ceti stars is larger than predicted by model atmospheres calculated with the ML1 version of the mixing-length theory (Ludwig, Jordan, & Steffen 1994).

In Figure 4, the two kinds of masses listed in Table 1 are plotted against each other. A different symbol is used for each reference for the gravitational redshifts, and stars cooler than $T_{eff} = 12{,}000$ K are shown as filled symbols. It is immediately apparent that the scatter is much larger than was apparent for the 11 generally bright stars in the original BSL sample (see Fig. 8 of BSL). In Figure 5, the differences between the spectroscopic and redshift masses are plotted against log T_{eff}, the latter taken from the spectroscopic determinations. Despite the increased scatter, especially at low temperatures, one can see from both figures that the mean masses between the two methods remain in generally good agreement. In Table 2 we list both the simple and weighted averages of the 43 entries of Table 1 (with optical spectra available), and those of subsets divided into temperature groups. Also listed are the (unweighted) standard deviations (σ_{rms}), the errors of the

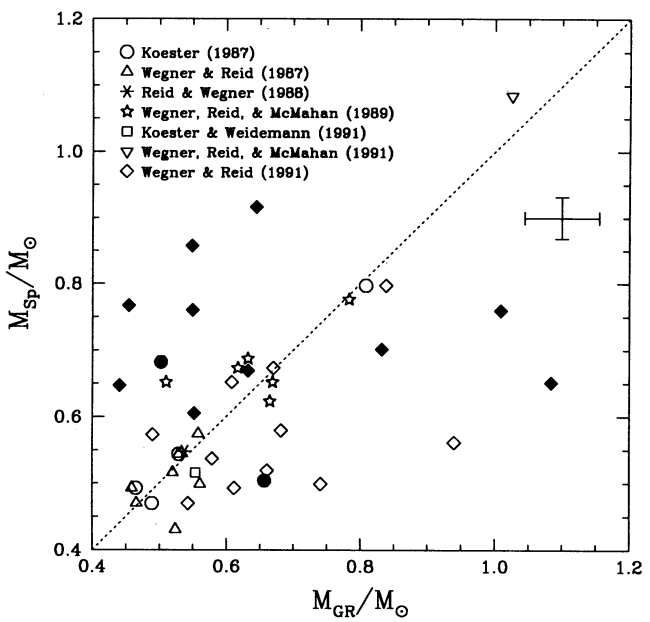

FIG. 4.—Spectroscopically determined masses plotted against those determined from published gravitational redshifts, using in both cases the evolutionary models of Wood (1990) for pure carbon interiors. The key identifies the symbols used for each reference for the gravitational redshift measurements; filled symbols indicate stars with $T_{eff} < 12{,}000$ K. Stars with two redshift determinations are plotted twice. The mean errors calculated from Table 1 are also indicated on the plot.

[3] Koester et al. (1994) adopted the ML1 version of the mixing-length theory with $\alpha \equiv l/H = 2$, where l is the mixing length and H is the pressure scale height. This parameterization is comparable to the ML2 version with $\alpha = 1$.

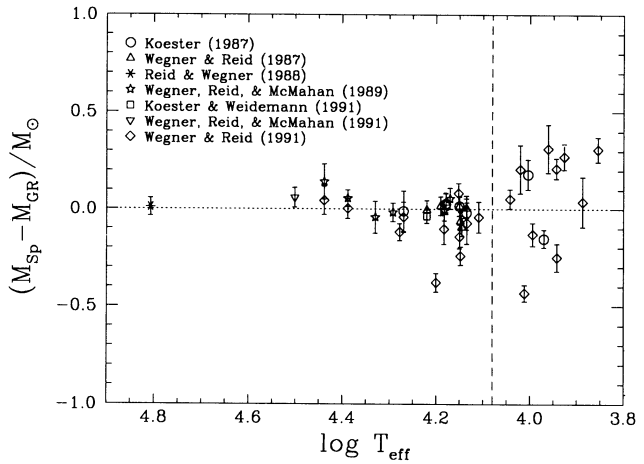

FIG. 5.—Difference between the spectroscopic and gravitational redshift masses plotted against log T_{eff}, as determined from the line fits. The vertical dashed line is located at T_{eff} = 12,000 K. The uncertainties of the mass difference are displayed as well. The same symbols are used as in Fig. 4 for the redshift references.

(weighted) mean (σ_M), and the number of entries in each subset. Table 3 lists the same results for the WR91 sample only. Several conclusions can be drawn from these figures.

First, the spectroscopic standard deviations, σ_{rms}, for all subsets of the complete sample (Table 2) are in excellent agreement with the value of $\sigma_{rms} = 0.137\ M_\odot$ obtained by BSL for their sample of 129 DA stars; we note that this dispersion is an intrinsic property of the mass distribution of white dwarfs. The gravitational redshift standard deviations are in good agreement with the BSL value as well, with the exception of the subset below 12,000 K for which the dispersion is significantly larger (0.210 $M_\odot$). We note that 10 of 12 stars in this subset come from the WR91 analysis; when only these 10 objects are considered, the standard deviation further increases to a value of 0.225 $M_\odot$ (see Table 3). This result is also apparent in Figure 4, where the dispersion in masses obtained from gravitational redshift measurements is much larger than that of the spectroscopic masses for objects below 12,000 K (filled diamonds). For

TABLE 2

COMPARISON OF MASS ESTIMATES

A. UNWEIGHTED AVERAGE[a]

Sample	$\langle M_{GR}\rangle/M_\odot$	σ_{rms}	$\langle M_{Sp}\rangle/M_\odot$	σ_{rms}	N
All stars	0.632	0.160	0.626	0.137	43
$T_{eff} > 12{,}000$ K	0.622	0.140	0.593	0.134	31
$T_{eff} \le 12{,}000$ K	0.658	0.210	0.710	0.111	12
Without WR91	0.594	0.136	0.601	0.148	22

B. WEIGHTED AVERAGE[b]

Sample	$\langle M_{GR}\rangle/M_\odot$	σ_M	$\langle M_{Sp}\rangle/M_\odot$	σ_M	N
All stars	0.656	0.006	0.603	0.005	43
$T_{eff} > 12{,}000$ K	0.615	0.007	0.577	0.005	31
$T_{eff} \le 12{,}000$ K	0.779	0.013	0.699	0.010	12
Without WR91	0.590	0.008	0.583	0.006	22

[a] $\langle M\rangle = \frac{1}{N}\sum_{i=1}^{N} M_i;\quad \sigma_M^2 = \frac{1}{N-1}\sum_{i=1}^{N}(M_i - \langle M\rangle)^2.$

[b] $\langle M\rangle = \sum_{i=1}^{N}\frac{M_i}{\sigma_i^2}\Big/\sum_{i=1}^{N}\frac{1}{\sigma_i^2};\quad \sigma_M^2 = \left(\sum_{i=1}^{N}\frac{1}{\sigma_i^2}\right)^{-1}.$

TABLE 3

COMPARISON OF MASS ESTIMATES FOR THE WR91 SUBSET

A. UNWEIGHTED AVERAGE

Sample	$\langle M_{GR}\rangle/M_\odot$	σ_{rms}	$\langle M_{Sp}\rangle/M_\odot$	σ_{rms}	N
All stars	0.672	0.177	0.652	0.124	21
$T_{eff} > 12{,}000$ K	0.669	0.131	0.578	0.096	11
$T_{eff} \le 12{,}000$ K	0.674	0.225	0.733	0.098	10

B. WEIGHTED AVERAGE

Sample	$\langle M_{GR}\rangle/M_\odot$	σ_M	$\langle M_{Sp}\rangle/M_\odot$	σ_M	N
All stars	0.751	0.010	0.630	0.007	21
$T_{eff} > 12{,}000$ K	0.689	0.015	0.565	0.009	11
$T_{eff} \le 12{,}000$ K	0.812	0.014	0.729	0.011	10

$T_{eff} > 12{,}000$ K, however, the WR91 subset yields a standard deviation of 0.131 $M_\odot$, a value which compares well with that of BSL. In contrast, the spectroscopic dispersions of the WR91 subset are identical below (0.098 $M_\odot$) and above 12,000 K (0.096 $M_\odot$). This comparison suggests that the redshift velocities from the WR91 subset probably suffer from larger uncertainties below 12,000 K that contribute to increasing the dispersion, in addition to the intrinsic spread in mass. The latter result is also obvious from Figure 5.

Second, the spectroscopic weighted and unweighted averages are in good agreement, both in Tables 2 and 3, as a result of the spectroscopic mass uncertainties being almost identical for all objects ($\sim$0.03 $M_\odot$). A similar conclusion applies to the redshift determinations, except for stars below 12,000 K for which the velocity uncertainties vary considerably from star to star. Consequently, the unweighted averages are significantly different from the weighted values for this subset, and the latter determinations are to be preferred. In the following, we thus consider only the weighted means. By definition, the errors of the mean in Tables 2 and 3 (σ_M) can be used to assess whether the difference in average mass from both techniques is significant. For the subset "Without WR91" in Table 2, the mean masses agree well within 1 σ, where the 1 σ value is calculated as $[\sigma_M(\mathrm{Sp})^2 + \sigma_M(\mathrm{GR})^2]^{1/2} \sim 0.01\ M_\odot$. Since this subset excludes all but two objects below T_{eff} = 15,000 K, the excellent agreement in masses indicates that the theoretical assumptions of the model calculations used in BSL are sound. If these two cool objects are excluded, the mean masses agree within 0.5 σ.

Third, when the WR91 sample alone is considered, the weighted average mass derived from gravitational redshifts is larger than the spectroscopic average by $\sim$10 σ. This large discrepancy is also responsible for the $\sim$6 σ difference when the entire sample in Table 2 is considered. In both Tables 2 and 3, the average gravitational redshift mass below 12,000 K is significantly *larger* by $\sim$5 σ than the spectroscopic mean mass, a result which is at odds with the fact that spectroscopic masses represent *upper* limits. Even more puzzling, the mass difference between both techniques for the WR91 subset is actually larger ($\sim$7 σ) for stars with $T_{eff} > 12{,}000$ K than for cooler objects. These results strongly suggest that there is a systematic problem with the WR91 determinations. Of particular concern to us are two cool stars (G116-16 and G121-22) with gravitational mass estimates above one solar mass, while the spectroscopic determinations are much lower (and could be even lower if one allows some helium to be present in their atmospheres). In previous papers (cf. Schmidt et al. 1992) we

have emphasized that abnormally high and low mass white dwarfs are obvious from the appearance of the line spectra—with abnormally broad profiles and a steep Balmer decrement in the case of the former. In Figure 2, we illustrate that line profiles and fit to G121-22, for which the redshift mass is 1.084 $M_\odot$, but with a spectroscopic mass of 0.651 $M_\odot$, only modestly higher than the BSL mean. The spectral features associated with high mass are simply not observed here. In contrast, we show the fit to G67-23 (*not* in this sample) which has a similar $T_{\rm eff}$ but a higher inferred spectroscopic mass. The difference is obvious; note in particular the broader profiles and weakness of the quenched high Balmer lines in the latter star.

Now we have already mentioned the difficulties in applying the spectroscopic method to the cooler stars, in particular those such as G121-22, which lie below the red edge of the ZZ Ceti instability strip. It is not necessarily our contention that the spectroscopic method yields the mass of G121-22 to the accuracy of objects in the BSL sample, or even that the method is intrinsically more accurate than using gravitational redshifts. We have already noted that the WR91 sample includes most stars for which the discrepancies are large, and this sample, unfortunately, is the source of a large fraction of the cooler stars. Therefore, we cannot yet use gravitational redshift measurements to better understand the systematic problems with the physics of cool white dwarf models, one of the goals of our project (see § 1), or to obtain independent mass estimates which could be used in turn to derive helium abundances for the individual objects.

Nevertheless, the results of Table 2 indicate that the cooler stars *appear* to have spectroscopic masses $\sim 0.1\ M_\odot$ larger than the hotter ones, a result which led Bergeron et al. (1990) to conclude that convective mixing had occurred in the atmosphere of these stars. Indeed, such large masses can be accounted for by assuming that these cool white dwarfs have atmospheres polluted by significant amounts of helium. Note that in the present calculations, we do take into account the nonresonant broadening described by Hammond et al. (1991), a process which had been incorrectly neglected in the earlier model calculations of Bergeron et al. (1990, 1991). The present results thus indicate that the conclusions of Bergeron et al. (1990) are not affected by these improved calculations.

4. DISCUSSION OF THE WR91 SAMPLE

The WR91 sample may in fact be subject to much larger errors than the other redshift studies listed in Table 1—perhaps even larger than the error estimates. Multiple measurements of the gravitational redshift velocity for a same star (see Table 1) indeed support this conclusion. Figure 6 displays a comparison of these multiple measurements, with the WR91 determinations shown as filled circles and plotted in abscissa ($v'_{\rm GR}$); note that all stars shown in Figure 6 have $T_{\rm eff} > 12{,}000$ K. Although measurements from various studies are in excellent agreement, the WR91 velocities are in general larger than previous determinations. In the remainder of this section, we offer some possible explanations for the problems encountered with the WR91 determinations.

The average apparent magnitude of the 21 stars we analyzed in common with WR91, using photometry catalogued by McCook & Sion (1987), is $V = 15.80$. This compares with $V = 13.00$ and 14.37 for the samples in common with Wegner & Reid (1987) and Wegner, Reid, & McMahan (1989), respectively. Hence, the fainter apparent magnitudes could account for the larger stated errors. One may also speculate that a

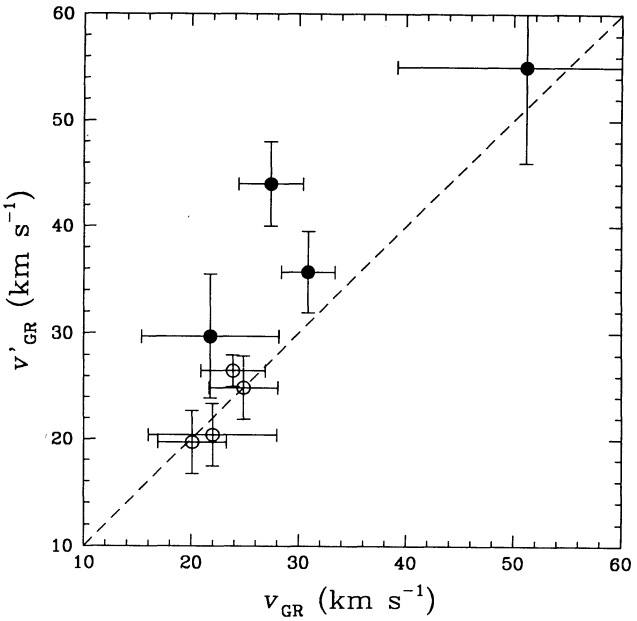

FIG. 6.—Comparison of gravitational redshift velocities for stars with multiple measurements, taken from Table 1. Stars with determinations by WR91 are shown as filled circles and their value are plotted in abscissa ($v'_{\rm GR}$). All stars have $T_{\rm eff} > 12{,}000$ K.

potential systematic error might affect fainter stars more than brighter ones. For instance, due to the faintness of the objects, WR91 used a resolution of 1.1 Å, ~3 times that of Wegner & Reid (1987) and Koester (1987). Thus WR91 barely resolve the non-LTE line core of Hα. Unlike most previous determinations, WR91 also measured Hβ as well as Hα. Grabowski, Madej, & Halenka (1987) have shown that Hβ is far more affected by pressure shifts than is Hα (see especially their Figs. 4 and 9); moreover, measurements of profiles at coarser resolution forces one to work farther from the line center, where pressure shifts quickly become important, especially in cool, high-gravity stars. The best procedure is probably just to measure the non-LTE core of the Hα line, ignoring the wings (or correcting for pressure shifts). We note also that the sense of a pressure shift is to increase the apparent gravitational redshifts and inferred masses, exactly the direction of the discrepancy between gravitational and spectroscopic determinations in Table 3B and Figure 6.

WR91 selected candidates from two sources: 14 stars in their total sample of 37 objects are common proper motion (CPM) pairs published by Oswalt, Hintzen, & Luyten (1988), all of which are part of the Luyten CPM catalogs (cf. Luyten 1979a, b). Here the fact that the proper motion of one component is the same as the other within the measurement errors is used to assert that they are a physical pair. Tables 1 and 2 of WR91 indicate that four of 14 Luyten stars[4] are probably nonphysical pairs due to the discordant velocities between both components of the system. This result is at odds with the conclusions of Oswalt et al. (1993) who showed that nearly all CPM pairs from Luyten catalogs with proper motions greater than 0.″1 yr^{-1} have photometric parallaxes and spectral types consistent with physical association. Given our additional con-

[4] Note that in Table 2 of WR91, G201-39/40, and GL905A/B are also Luyten pairs named LP 135-154/155 and LP 347-4/5, respectively (see Oswalt et al. 1988).

cerns with the WR91 discussed above, it is possible that some, if not all four of the rejected systems are physically associated. Furthermore, one needs to be cautious when ruling a pair nonphysical on the basis of a single velocity measurement.

The remaining 23 objects in the WR91 sample come from the EG lists (see WR91 and references therein) which contain mainly stars from the Lowell Observatory proper motion catalogs (cf. Giclas, Burnham, & Thomas 1971). Many of these pairs, and most notably the "B" pairs, represent optical double stars found to have contrasting colors—i.e., possible pairings of a white dwarf with a late-type main sequence star—but without clear evidence for common proper motion. Eggen & Greenstein and Oswalt (1981) found that a large fraction of the Giclas "B" pairs are not physically associated. Although an examination of Tables 1 and 2 from WR91 reveals that nonphysical pairs (or pairs containing a subdwarf) are as common within the Giclas pairs (seven of 23) than within the Luyten pairs (four of 14; see comment above, however), it is likely that a few of those "B" pairs accepted by WR91 are nonphysical pairs as well, with velocity differences yielding plausible but erroneous gravitational redshifts. Finally we note that USNO measurements (Harrington & Dahn 1980) of the common proper motions and trigonometric parallaxes of the G117-B15A/B system discussed above are well within 1 σ uncertainty, and this pair is undoubtedly physically associated.

In conclusion, it is clear that more and necessarily fainter white dwarfs in binary systems and clusters will have to be observed for gravitational redshifts before the cross-comparison with stellar spectral analyses can achieve all of the goals outlined in the Introduction. Even with the 5 m Palomar telescope, WR91 have encroached on the magnitude limit for which their measurement errors exceed the demanding several km s^{-1} accuracy required for reasonably accurate mass determinations. We hope in fact that our paper motivates researchers to tackle these and fainter stars with the Keck 10 m or other large telescopes of the future.

We are extremely grateful to the referee, Terry Oswalt, for his comments and suggestions which helped to improve significantly the interpretation of our results. J. L. acknowledges the National Science Foundation grant AST 92-17961. PB was supported in part by NSERC Canada, and by the Fund FCAR (Québec).

REFERENCES

Adams, W. S. 1925, Observatory, 36, 2
Bergeron, P. 1993, in White Dwarfs: Advances in Observation and Theory, NATO ASI Ser., ed. M. A. Barstow (Dordrecht: Kluwer), 267
Bergeron, P., Saffer, R. A., & Liebert, J. 1992a, ApJ, 394, 228 (BSL)
Bergeron, P., Wesemael, F., Beauchamp, A., Wood, M. A., Lamontagne, R., Fontaine, G., & Liebert, J. 1994, ApJ, 432, 305
Bergeron, P., Wesemael, F., & Fontaine, G. 1991, ApJ, 367, 253
———. 1992b, ApJ, 387, 288
Bergeron, P., Wesemael, F., Fontaine, G., & Liebert, J. 1990, ApJ, 351, L21
Bergeron, P., Wesemael, F., Lamontagne, R., Fontaine, G., Allard, N. F., & Saffer, R. A. 1995, ApJ, submitted
Giclas, H. L., Burnham, Jr., R, & Thomas, N. G. 1971, The G Numbered Stars (Northern Hemisphere) (Flagstaff AZ: Lowell Obs.)
Grabowski, B., Madej, J., & Halenka, J. 1987, ApJ, 313, 750
Greenstein, J. L., Boksenberg, A., Carswell, R., & Shortridge, K. 1977, ApJ, 212, 186
Greenstein, J. L., & Trimble, V. 1967, ApJ, 149, 283
Hammond, G. L., Sion, E. M., Kenyon, S. J., & Aannestad, P. A. 1991, in Proc. 7th European Workshop on White Dwarfs, NATO ASI Ser., ed. G. Vauclair & E. M. Sion (Dordrecht: Kluwer), 317
Harrington, R. S., & Dahn, C. C. 1980, AJ, 85, 454
Hummer, D. G., & Mihalas, D. 1988, ApJ, 331, 794
Koester, D. 1987, ApJ, 322, 852
Koester, D., Allard, N. F., & Vauclair, G. 1994, A&A, 291, L9
Koester, D., & Weidemann, V. 1991, AJ, 102, 1152
Ludwig, H.-G., Jordan, S., & Steffen, M. 1994, A&A, 294, 105
Luyten, W. J. 1979a, The LHS Catalogue (2d. ed.; Minneapolis: Univ. of Minnesota)
———. 1979b, The NLTT Catalogue (Minneapolis: Univ. of Minnesota)
McCook, G. P., & Sion, E. M. 1987, ApJS, 65, 603
Oswalt, T. D. 1981, Ph.D. thesis, Ohio State Univ.
Oswalt, T. D., Hintzen, P. M. N., & Luyten, W. J. 1988, ApJS, 66, 391
Oswalt, T. D., Smith, J. A., Shufelt, S., Hintzen, P. M., Leggett, S. K., Liebert, J., & Sion, E. M. 1993, in White Dwarfs: Advances in Observation and Theory, NATO ASI Ser., ed. M. A. Barstow (Dordrecht: Kluwer), 419
Reid, N., & Wegner, G. 1988, ApJ, 335, 953
Schmidt, G. D., Bergeron, P., Liebert, J., & Saffer, R. A. 1992, ApJ, 394, 603
Wegner, G., & Reid, I. N. 1987, in IAU Colloq. 95, The 2d Conf. on Faint Blue Stars, ed. A. G. Davis Philip, D. S. Hayes, & J. Liebert (Schenectady: L. Davis), 649
———. 1991, ApJ, 375, 674 (WR91)
Wegner, G., Reid, I. N., & McMahan, R. K. 1989, in IAU Colloq. 114, White Dwarfs, ed. G. Wegner (New York: Springer), 378
———. 1991, ApJ, 376, 186
Wood, M. A. 1990, Ph.D. thesis, Univ. of Texas at Austin